Materials and Structures (2017)50:7
DOI 10.1617/s11527-016-0887-4

ORIGINAL ARTICLE

Production methods for reliable construction of ultra-high-performance concrete (UHPC) structures

Libya Ahmed Sbia · Amirpasha Peyvandi · Jue Lu · Saqib Abideen · Rankothge R. Weerasiri · Anagi M. Balachandra · Parviz Soroushian

Received: 17 August 2015 / Accepted: 21 May 2016

Abstract Mix design procedures were developed around the core strategy of maximizing the packing and ensuring distributed size distribution of the particulate matter in UHPC for achieving ultra-high strength levels and desired fresh mix workability using locally available materials and concrete-making facilities. The linear density packing model and the continuously graded particle packing model provided the theoretical basis for proportioning the UHPC mixtures. Criteria were devised for selection of local materials to be used in UHPC structures. Experimental investigations were conducted in order to refine and optimize the UHPC mix proportions, yielding the targeted compressive strength of 200 MPa (30 ksi). The final UHPC mix design developed in the study was used for pilot-scale production of a large 1 m × 1 m × 1 m (3.3 ft × 3.3 ft × 3.3 ft) reinforced concrete block, with UHPC batched in a ready-mixed concrete plant and mixed/transported using a conventional concrete truck (transit mixer).

Keywords Ultra-high-performance concrete (UHPC) · Mix design · Conventional concrete aggregates · Packing density

L. A. Sbia · P. Soroushian
Department of Civil and Environmental Engineering, Michigan State University, 3546 Engineering Building, E. Lansing, MI 48824-1226, USA
e-mail: Sbialiby@msu.edu

P. Soroushian
e-mail: Soroushi@egr.msu.edu

A. Peyvandi (✉)
Structural Department, Stantec, 500 Main St., Baton Rouge, LA 70801, USA
e-mail: Amirpasha.peyvandi@gmail.com

J. Lu · S. Abideen · R. R. Weerasiri · A. M. Balachandra
Metna Co., 1926 Turner St., Lansing, MI 48906, USA
e-mail: Juelu66@yahoo.com

S. Abideen
e-mail: Sametnaco@gmail.com

R. R. Weerasiri
e-mail: Sametnaco@gmail.com

A. M. Balachandra
e-mail: Abmetnaco@gmail.com

Published online: 04 August 2016

1 Introduction

Ultra-high performance concrete (UHPC) refers to a class of cementitious composites with outstanding material properties. UHPC provides superior compressive, tensile and flexural strengths, ductility, toughness, and diffusion and abrasion resistance [1]. The enhanced properties of UHPC are realized by increasing the packing density of cementitious and filler constituents, use of low water/binder (*W*/*C*) ratios, and effective use of fibers [2]. Traditional methods used for design and production of UHPC generally emphasize removal of coarse aggregates, use of specially graded fine aggregates at relatively

low dosages, use of high superplasticizer (high-range water reducer) and silica fume contents, and curing at elevated temperatures [3].

Field applications of UHPC have largely emphasized production of precast/prestressed concrete elements [4–10], and repair/rehabilitation of concrete structures [11]. The trends toward field (including cast-in-place) applications have highlighted some issues which need to be addressed before UHPC can emerge as a mainstream construction material. The UHPC performance characteristics are more sensitive than those of normal- and high-strength concrete to the specifics of the raw materials (e.g., aggregates) composition and geometric attributes [10, 12], the details of casting and consolidation practices [13–15], and the curing and early-age exposure conditions [2, 10, 16]. Tailoring of the UHPC mix design to enable use of locally available materials, and refinement of the construction and quality control practices would be needed for reliable field production of UHPC structures. While there is growing evidence supporting the favorable life-cycle economy and sustainability of UHPC structural systems [17, 18], evolution of UHPC into a mainstream construction material would be impacted by initial cost considerations which would benefit from lowering the cementitious binder content of UHPC [19].The relatively high packing density of UHPC and the use of micro/nanoparticles increase the mixing energy [20–25] and duration and necessitate use of special mixing equipment for production of homogeneous UHPC mixtures [26]. Market acceptance of UHPC would benefit from development of mixtures which can be prepared using the drum and pan mixers commonly used by the concrete industry.

Existing UHPC materials employ distinctly fine aggregates together with special equipment and methods which are not commonly available to the concrete industry. UHPC has its roots in development of specialty cementitious materials such as reactive powder concrete [27], which employ materials and methods suiting factory production (similar to ceramics). This deep-rooted tradition has been followed in most developments in the field of UHPC. There is a need to re-evaluate this approach if UHPC is to be embraced by the concrete industry. Fortunately, developments in UHPC have laid a solid scientific foundation for mix design using the packing density [18] and the mortar thickness [28] models, which could be employed towards design of UHPC with conventional materials.

The purpose of this study is to develop guidelines for proportioning locally available particulate (granular) matter (including cement, silica fume, other supplementary cementitious materials, aggregates, fibers, and optionally commonly available powder) for achieving a dense particle packing without compromising the potential for achieving desired fresh mix characteristics with UHPC.

2 Materials and methods

2.1 Materials

This study used readily available natural sand from Michigan, USA (MI) and New Mexico (NM), USA as fine aggregates in UHPC, and silica sand was used occasionally to improve the packing density of particulate matter. Fineness moduli ranging from 2.5 to 3.2 are recommended for the fine aggregates used in high-strength concrete in order to realize desired fresh mix workability [29]. Existing UHPC mixture do not generally use coarse aggregates. This study used locally available crushed granite and limestone from mid-Michigan and New Mexico as coarse aggregate in UHPC. Different coarse aggregates were investigated, with emphasis placed on crushed granite (grading #67, 7 and 8) supplied by the Highland Plant of American Aggregate of Michigan Inc. (mid-Michigan) and Russell Sand & Gravel Co., Inc. Table 1 Shows the properties of crushed granite used in this study. Natural sands were supplied by High Grade Materials (Lansing, MI) and Russell Sand & Gravel Co., Inc. (Las Cruces, NM).

The MI and NM crushed granites with #6, 7 and 8 particle sizes, the maximum particle sizes of which are 18, 4.8 and 9.5 mm, respectively, were selected for use as coarse aggregates. MI and NM natural sands with #9 particle size with maximum particle size of 2 mm following literature studies were used as fine aggregates. The cement used in the project is ordinary Type I Portland cement, manufactured by Lafarge. Silica fume was provided by Norchem. Ground granulated blast-furnace slag (GGBFS) was supplied by the Lafarge South Chicago plant (Grade 100 Newcem). Quartz powder with an average particle size of 3.9 μm

Table 1 Properties of granite used in this study

Materials	Density (g/cm^3)	Absorption (%)	L.A. abrasion (%)	Theoretical compressive strength (MPa)
Granite (MI)	2.2	1.1	21.0	155.0
Granite (NM)	2.2	2.7	18.3	183.5

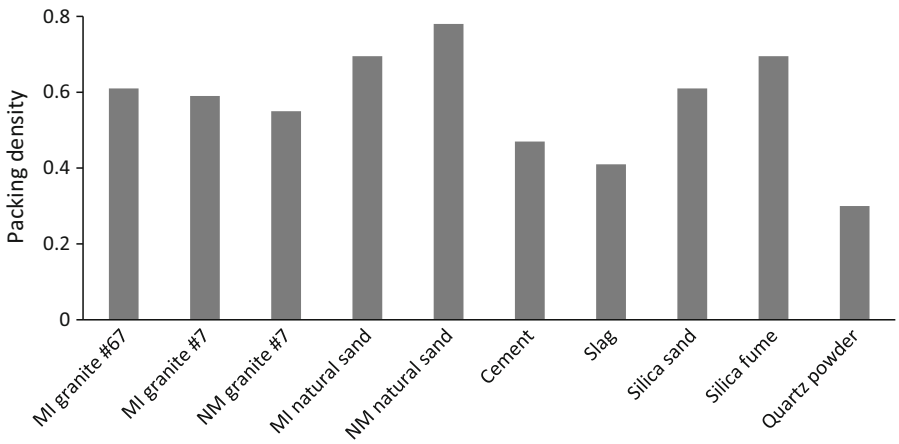

Fig. 1 Measured packing densities of the various particulate constituents used in UHPC

was provided by AGSCO Corporation, Illinois. Size distributions were assessed by sieve analysis, or provided by manufactures. The packing density of each particulate constituent was measured by weighing a 1-l container filled with the particles consolidated on a vibrating table over 2 min. Packing density of different particulate constituent presented in Fig. 1.

Two types of high-range water reducer (HRWR) were evaluated: ADVA® Cast 575 supplied by W.R. Grace, and Chryso Fluid Premia 150 supplied by Chryso Company, Charlestown, Indiana. Both HRWRs are polycarboxylate-based superplasticizers. ADVA® Cast 575 is a powerful dispersant admixture that meets the ASTM C494 Type F requirements at a dosage of 144 mL/100 kg (2.2 oz/cwt), and ASTM C1017 requirements at a dosage of 137 mL/100 kg (2.1 oz/cwt). Water reduction effects generally remain robust and linear as dosage rates are increased. ADVA® Cast 575 is, however, intended for self-consolidating concrete; it keeps the mix cohesive to avoid segregation. In application to UHPC mixtures, where the relatively high dosage of silica fume produces a highly cohesive mix, ADVA® Cast 575 did not produce desired flowability. Chryso Fluid Premia 150, on the other hand, is recommended for all concrete mixtures; it was found to be particularly effective in UHPC mixtures where high flowability is required to enable convenient mixing and handling of the cohesive mix.

The steel fibers used initially in UHPC mixtures were straight, brass-coated with 13 mm (0.5 in) length and 0.175 mm (0.007 in) diameter. A rather similar straight, brass-coated steel fibers with 13 mm (0.5 in) length and 0.2 mm (0.008 in) diameter with a tensile strength of between 690 and 1000 MPa (96,600 and 140,000 psi) and a modulus of elasticity of 210,000 MPa (30,457 ksi), according to the manufacturer was used after preliminary studies. Hooked steel fibers with 30 mm (1.2 in) length and 0.5 mm (0.02 in) diameter were also evaluated in UHPC mixtures.

Models and criteria were developed, as described in the following sections, for selection and proportioning of the particulate matter (as the granular skeleton) in UHPC. However, compressive strength was the focus of this study and all characteristics then evaluated to meet following criteria.

2.2 Performance target of UHPC

These models and criteria were complemented with guides developed empirically for selection of water/binder ratio, chemical admixtures and fibers in order to design UHPC mixtures which target the following

performance requirements (for construction of large UHPC structures) [9, 17, 30, 31]: (i) >200 MPa (30 ksi) compressive strength; (ii) >20 MPa (3 ksi) split cylinder tensile strength; (iii) >35 MPa (5.8 ksi) modulus of rupture; (iv) strain-hardening behavior; (v) <0.01 ml/(m^2 s) initial surface sorption (10 min); (vi) <200,000 kJ/m^3 cumulative heat of hydration; (vii) <300 μm/m autogenous plus drying shrinkage; and (viii) >500 mm (20 in) fresh mix spread and >200 mm (8 in) slump.

2.3 Methods

The relatively high packing density of UHPC mixtures increases the energy and time required for their thorough mixing [20]. So far, UHPC mixes have not been mixed in rotary drum mixers which simulate the action of transit and central mixers commonly used in ready-mixed concrete plants. Examples of mixers used for reducing the inhomogeneity of UHPC mixtures and lowering their mixing time include: (i) intensive mixer with inclined drum and variable tool speed; (ii) paddle mixer (iii) planetary mixer; and (iv) pan mixer. Three mixer types were evaluated for production of the new UHPC mixtures developed in the study; the objective here is to explore the possibility of employing a simple drum mixer which simulates the action of the transit and central mixers commonly used in ready-mixed concrete plants. The three mixers considered in the study included: (i) a 0.02 m^3 planetary mixer (Hobart A-200); (ii) a 0.08 m^3 capacity pan mixer (CollomixCollomatic TMS 2000 Compact Mixer); and (iii) a drum mixer. UHPC mixtures were initially prepared using the planetary mixer, and some mixes with desirable fresh mix workability and hardened material compressive strength were selected for mixing in the pan and eventually the drum mixer.

The following UHPC mixing sequence was selected based on trial-and-adjustment studies:

1) Dry blend all granular materials, including aggregates, cement, silica fume, slag, and quartz powder (1 min).
2) Sprinkle steel fibers onto the dry mix, and thoroughly mix all the ingredients (1 min).
3) Mix water and superplasticizer, add half of the solution to the pre-blended granular matter, and mix for 1 min.
4) The remaining of the water/superplasticizer solution second half added gradually over a period of 1 min.
5) Continue mixing until a homogeneous mix with stable workability is achieved (4–5 min).

Initial efforts were focused on design of UHPC mixtures which offer a desired balance of fresh mix workability and early-age (after thermal curing) compressive strength. Fresh mix workability was assessed using the flow table test following ASTM C230 procedures. Following standards, the table top and inside of the mold need to be wetted and cleaned, mold need to be filled with concrete in two layers. The mold then removed from the concrete by a steady upward pull. The table raised and dropped from a height of 12.5 mm, 15 times in about 15 s (dynamic test) then the diameter of the spread concrete need to be read and reported. In static test, there is no dropping and diameter of concrete after mold removal need to be reported. Compression tests were performed on 76 mm (3 in) diameter and 152 mm (6 in) height cylinders consolidated on a vibrating table. The cylinders were held under a wet cloth at room temperature for 24 h, after which they were demolded and subjected to two alternative thermal (steam) curing methods: (i) 90 °C over 48 h; and (ii) 70 °C over 72 h. After thermal curing and cool-down to room temperature, the specimens were stored at room temperature and 50 % relative humidity in order to equilibrate their moisture content. Initial tests for tailoring the material selections and mix proportions were performed at 7 days of age. Both ends of compression test specimens (3 specimens were made for each compression test) were ground to produce flat loading surfaces. Length, diameter and density of each specimen were measured prior to performance of compression tests.

3 Development of UHPC mix design procedures

3.1 Packing density of UHPC

Design of a dense granular structure constitutes the foundation for design of UHPC mixtures. The granular structure in UHPC should yield a desired balance of rheological attributes, packing density, and chemical reactivity of constituents. A number of packing models [28, 32] are available, including: (i) the linear

packing density model (LPDM) for grain mixtures; (ii) the solid suspension model (SSM); and (iii) the compressive packing model (CPM). LPDM has been used successfully towards prediction of the optimal proportions of concrete, though its linear nature implies some drawbacks [28]. Equations derived based on LPDM for prediction of the packing density (c) are presented below [28]:

$$c = \min(c(t)) \text{ for } y(t) > 0, \text{ with} \tag{1}$$

$$c(t) = \frac{\alpha(t)}{1 - \int_d^t y(x) f(x/t)\mathrm{d}x - [1 - \alpha(t)] \int_t^D y(x) g(t/x)\mathrm{d}x} \tag{2}$$

$$f(z) = 0.7(1 - z) + 0.3(1 - z)^{12} \tag{3}$$

$$g(z) = (1 - z)^{1.3} \tag{4}$$

where, t is the size of grains, $y(t)$ is the volume size distribution of the grain mixture (having a unit integral: $\int_d^D y(x)\mathrm{d}x = 1$), d and D are, respectively, the minimum and maximum sizes of grains, $\alpha(t)$ is the specific packing density of the t-class, $f(z)$ is the loosening effect function, and $g(z)$ is the wall effect function. These functions, which describe binary interactions between size classes, are universal; $y(t)$ and $\alpha(t)$ were measured experimentally. The 4C-packing software (developed by the Danish Technological institute), which is based on LPDM, was used to predict the packing density of UHPC mixtures. In order to predict the packing density of aggregates or concrete mixtures using the 4C-packing software, material properties such as particle density, particle size distribution and specific packing density constitute the parameters input to the software.

Prior to optimizing the UHPC mix proportions for maximizing packing density, aggregates alone were proportioned to maximize their packing density and minimize void content. This lowering of void content between aggregate particles benefits the fresh mix workability of UHPC at a constant binder-to-aggregate ratio. This is because the binder content required to fill the voids between aggregates is minimized, leaving more of the binder content available for wetting and lubricating the aggregates (i.e., reduce the interparticle friction) and thus improving fresh mix workability. Figure 2 shows the packing density of aggregates predicted using the 4C-packing software. The packing density of NM aggregates is generally higher than the MI aggregates used here, which can be partly attributed to the lower fineness modulus of the NM natural sand (2.65) versus MI sand (2.90). Figure 2 also shows the measured values of packing density for MI aggregates; the experimental trends follow those predicted theoretically, noting that the experimental packing densities are 5 % higher than the theoretical values. Both theoretical and experimental packing densities indicate that fine aggregate contents of 45–50 vol% of total aggregate maximizes the packing density of aggregates; further increase of fine aggregate content lowers the fresh mix workability. These findings suggest that a fine aggregate content of 45 vol% in the blend of fine and coarse aggregates is a reasonable choice.

Table 2 shows the initial UHPC mix designs, and their packing densities (predicted by the 4C-packing software). Mix #1 (has 55 vol% crushed granite and 45 vol% natural sand; the binder comprises 70 % cement, 10 % silica fume and 20 % slag. The predicted packing density of Mix #1 is 0.723. In Mix #2, where the silica fume content of binder was increased to 20 %, the slag content was decreased to 10 %, and quartz powder was introduced at 20 % of total binder content, packing density increased to 0.787, which is at a satisfactory level for UHPC. Packing density decreased in the case of Mix #3 where, when compared with Mix #2, the quartz content of binder was lowered to 10 %, and the slag content raised to 20 %.

3.2 Optimizing the graded particles

Besides a high packing density, a continuous particle size distribution which suits packing density also perfects the UHPC mix design. The grading of particulate matter influences both the fresh mix and hardened material properties [33]. One of the most commonly used ideal grading models is the (modified) Andreassen model. A commercially available particle packing software, EMMA, based on the Andreassen model was used to optimize particle size distribution for improved packing of the particulate matter. This software was used in conjunction with the 4C-packing software. The EMMA software calculates and displays the particle size distribution of a blend of particulate matter using the particle size distributions of the

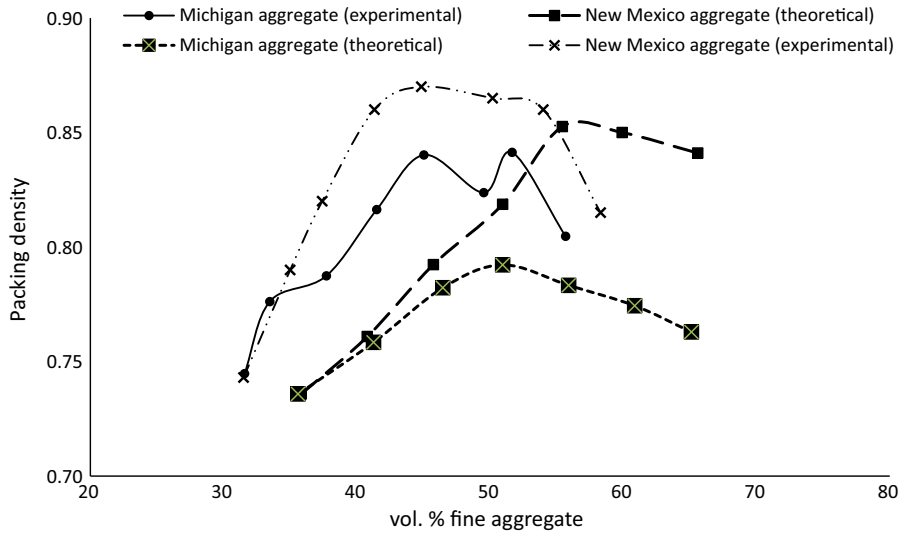

Fig. 2 Packing densities of blended coarse and finer aggregates versus the vol% of fine aggregate predicted by the 4C-Packing software or determined experimentally

Table 2 Initial UHPC mix designs (kg/m^3) and their predicted packing densities

Mix #	1	2	3
Total aggregates	1383.00	1383.00	1383.00
Crushed granite (#7)	772.37	772.37	772.37
Natural sand	610.63	610.63	610.63
Binder	1037.25	1037.25	1037.25
Cement	726.08	518.63	518.63
Silica fume	103.73	207.45	207.45
Slag	207.45	103.73	207.45
Quartz powder	–	207.45	103.73
Binder-to-aggregate ratio	0.75	0.75	0.75
Packing density	0.72	0.79	0.78

constituents as input, and compares the resulting particle size distribution against the 'ideal' distribution based upon the Andreassen model [34]. Andreassen suggested that optimal packing occurs when the particle size distribution can be described by the model:

$$CPFT = (d/D)^q 100 \quad (5)$$

where, CPFT is the 'cumulative (volume) percent finer than', d is particle size, D is the maximum particle size, and q is the distribution coefficient. It is possible to obtain 0 % voids (or 100 % packing) if q is equal to or less than 0.37 [35]. The modified Andreassen model, which considers a minimum particle size, is expressed as follows:

$$CPFT = [(d^q - dm^q)/(D^q - dm^q)] \quad (6)$$

where, dm is the minimum particle size. The term 'q' or 'q-value' increases with increasing amount of coarse materials, and decreases with increasing amount of fine materials. A more detailed description of the two models and the software algorithms is presented in the EMMA User Manual [34]. A mix with a lower distribution modulus, q, will result in a fine aggregate mix, whereas a high q value will result in a coarse mix. The packing factor and compressive strength decrease with increasing distribution modulus [36]. Past investigations have shown that q values of 0.25–0.30 may be used to design high-performance concrete, and that q values less than 0.23 yield more workable concrete mixtures [37].

A number of UHPC mix designs are presented in Table 3, and the corresponding size gradations (of their particulate matter) are presented in Fig. 3. The 'traditional' UHPC mix is shown in Fig. 3 to fit the modified Andreassen model curve with $q = 0.25$, but with <1000 μm particle size because silica sand is the only aggregate used in this mix. A modified UHPC mix design developed by Wang et al. [30]. was also examined. This UHPC mix clearly deviates from the model curve; in spite of this, its compressive strength reached 180 MPa (26 ksi) at 180 days. The original mix design (UHPC-A1) seems to fit the model curve with $q = 0.12$, but with some deviations. Therefore, tailored UHPC mix designs were developed by tailoring the dosages of some particle sizes to achieve

Table 3 Optimum mix designs developed based on continuously graded particle size distribution model yielding high packing densities

Mix designation	Wang et al. [28]	UHPC-A1	Ideal 1	Ideal 2	Ideal 3	Ideal 4	Traditional (commercial) UHPC
Total aggregates	1539.00	1383.00	1383.00	1383.00	1383.00	1383.00	1020.00
Crushed granite	923.00	772.37	691.50	772.37	553.20	525.54	–
Natural sand	616.00	610.63	691.50	610.63	553.20	553.20	–
Silica sand	–	–	–	–	276.60	304.26	1020.00
Binder ratio	0.58	0.75	0.75	0.65	0.75	0.75	1.13
Binder	900.00	1037.25	1037.25	898.95	1037.25	1037.25	1154.00
Cement	450.00	518.63	518.63	449.48	518.63	518.63	712.00
Silica fume	180.00	103.73	207.45	179.79	228.20	228.20	231.00
Slag	90.00	207.45	103.73	89.90	103.73	103.73	–
Quartz powder	180.00	207.45	207.45	179.79	186.71	186.71	211.00

a more distributed gradation which better fits the modified Andreassen curve. The optimized "Ideal 1" and "Ideal 2" mixes fit the modified Andreassen curves better than the original 'UHPC-A1' mix. These basic mixes, however, fell short in terms of particles in the 100–1000 μm size range; silica sand with size distribution in the range of 180–600 μm was thus incorporated into the 'Ideal 3' and 'Ideal 4' UHPC mix designs. As a result, the fit of combined grading to the model curve improved significantly.

3.3 Approach to UHPC mix proportioning

The packing density and ideal particle gradation models presented above provided a basis to develop an approach to mix proportioning of UHPC. A flowchart for the approach to UHPC mix design procedure is presented in Fig. 4. This flowchart was followed in design of UHPC mixtures considered in the experimental work.

4 Results and discussion

Initial efforts towards development of scalable UHPC mixtures were based upon some promising past efforts on UHPC formulations which represent a trend away from conventional UHPC mix designs. The reported mix designs are presented in Table 4 together with their compressive strengths; the first trial UHPC mix considered in this study ('UHPC-B1') is also introduced in Table 4.

An attempt was made to reproduce the successful UHPC mixes [30, 38, 39] (Table 4) as well as the first 'UHPC-B1'Trial mix (M), in Table 4, Three types of steel fibers were used, as follows: (i) hooked (H) with length of 30 mm (1.2 in) and diameter of 0.5 mm (0.02 in), providing an aspect ratio of 60; (ii) helix (HX) with 25 mm (1 in) length and 0.5 mm (0.02 in) diameter, providing an aspect ratio of 50; and (iii) straight (S) with length of 13 mm (0.5 in) and diameter of 0.2 mm (0.008 in), providing an aspect ratio of 65. The steel fiber volume fractions considered ranged from 1.0 to 2.0 %. Thermal curing (90 °C over 48 h) followed by storage at 50 % relative humidity and room temperature was employed. Figure 5 shows the resulting compressive strengths measured at 10 days of age. Reproductions of the promising mixtures from the literature did not yield satisfactory results (>150 MPa, 22 ksi compressive strength) to qualify as UHPC. The differences between these results and the compressive strengths of the original UHPC mixtures reported in the literature could be partly attributed to the differences in gradations, compositions and physical properties of aggregates and cementitious materials as well as the composition and effectiveness of superplasticizer. One of the 'UHPC-B1' variations (MH1.5 %) with 1.5 vol% hooked steel fibers, however, qualified as UHPC based on its 10-day compressive strength. The compressive strength of 'UHPC-B1' increased as the volume fraction of hooked steel fibers was raised from 1 % (MH1 %) to 1.5 % (MH1.5 %). This

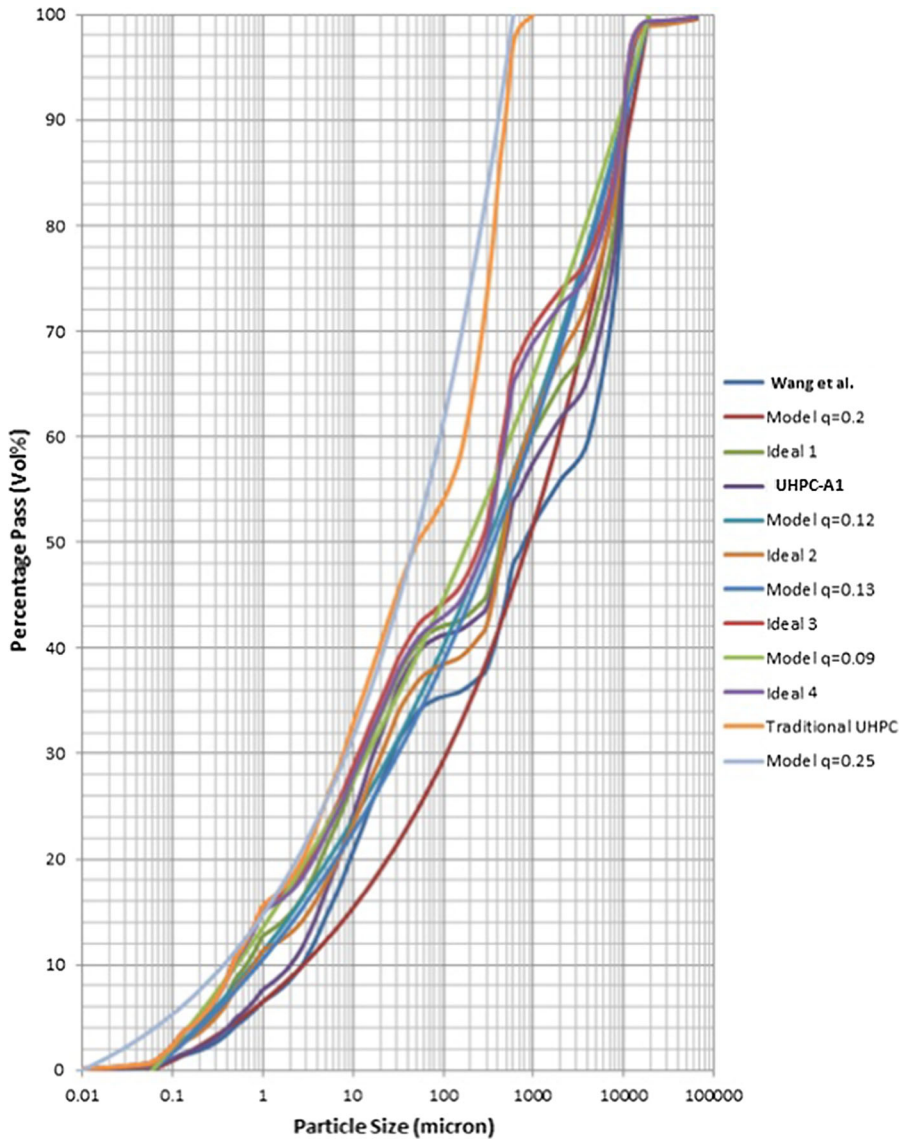

Fig. 3 Comparisons of the size distributions of the particulate matter in different UHPC mix designs with modified Andreassen curves

trend agrees with the findings of relevant background work, which indicate that the compressive strength of UHPC, unlike those of normal- and high-strength concrete materials, benefits from steel fibers. The initial 'UHPC-B1' mixtures used here were produced using the 'ADVA® Cast 575' superplasticizer (HRWR), which was found to make the UHPC more cohesive and thus less workable. Based on a comparison between different HRWRs, 'Chryso Fluid Premia 150' was found to better suit UHPC; this superplasticizer was used thereafter.

4.1 Optimization of water and HRWR

Given the dominant role of water and HRWR in controlling the UHPC workability, and the significant influence of water/binder ratio in the UHPC strength, development of Group #1 UHPC mixtures (Table 5) emphasized minimization of the water/binder ratio to increase compressive strength and provided adequate fresh mix workability. Based on the outcomes of initial trials presented in Fig. 5, hooked steel fibers with 30 mm (1.2 in) length and 0.5 mm (0.02 in)

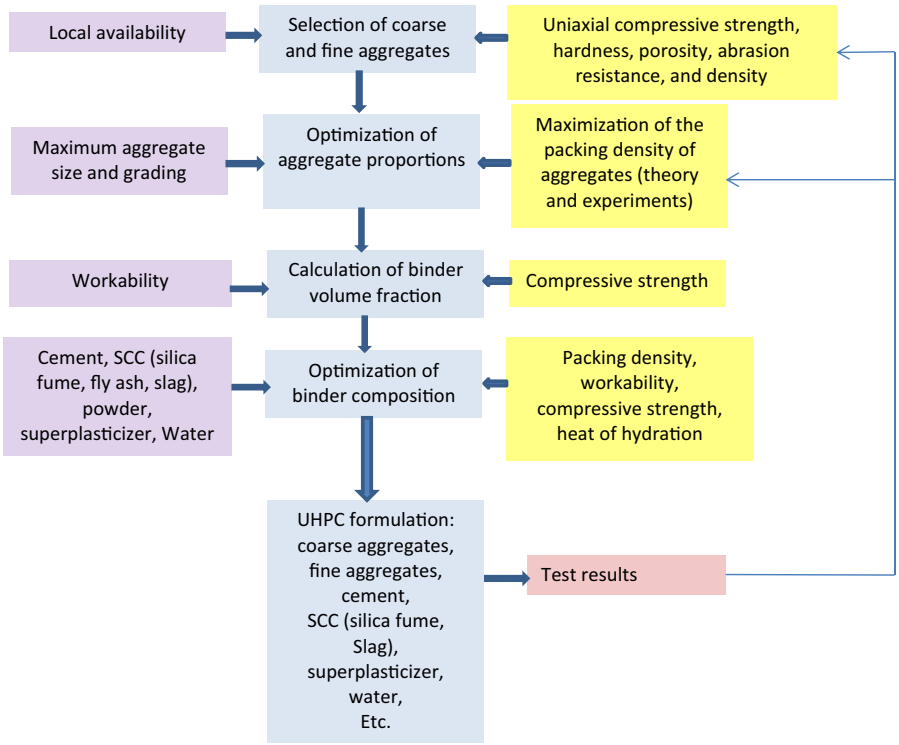

Fig. 4 Flowchart outlining the approach to UHPC mix design

Table 4 The more scalable UHPC mix designs (kg/m^3) reported in the literature, and the first trial mix considered in the project ('UHPC-B1')

Mix constituent	Ma and Schneider [37]	Wang et al. [28]	Maruyama et al. [36]	'UHPC-B1'
Aggregate	1020.0	1539.0	1383.0	1383.0
Coarse aggregates	715.2	923.0	932.0	772.4
Natural sand	304.1	616.0	451.0	610.6
Cementitious materials	804.9	900.0	1033.0	933.0
Cement	465.0	450.0	930.0	623.0
Slag/fly ash	–	180.0	–	103.0
Silica fume	140.0	90.0	103.0	207.0
Limestone (L)/quartz (Q) flour	199.0	180.0	–	–
Water	124.2	144.0	155.0	149.2
HRWR	16.3	18.0	26.9	39.4
Water/binder ratio	0.16	0.18	0.15	0.16
Compressive strength (MPa) (28 days)	149.2	174.5	173.2	–
Compressive strength (MPa) (365 days)	155.8	180.0	180.0	–

diameter were considered in these mixtures initially at 1.0 vol% ('UHPC-B2' & 'UHPC-B3'), and it is 1.5 vol% in 'UHPC-B4a' and 'UHPC-B4b' since the fresh mix workability of the first two mixtures was found to be desirable. The HRWR used at 25 wt% of water here (Chryso 150) produced substantially improved flowability at 0.16 water/binder ratio (. The 7- and 28-day compressive strengths of Group #1 mixtures (thermally cured following method explained earlier) are, however, within

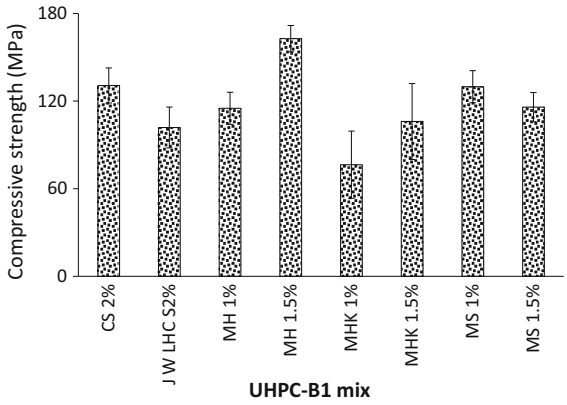

Fig. 5 Compressive strength test results (UHPC in preliminary laboratory studies (means and standard errors)

100–115 MPa (14–17 ksi range), which don't reach to the targeted compressive strength of >150 MPa (>22 ksi).

4.2 Steel fiber

The Group #2 mixtures (Table 6) focused on replacement of hooked steel fibers (with relatively large diameter) by the finer straight steel fibers with 0.17 mm (0.007 in) diameter and 13 mm (0.5 in) length. The relatively high specific surface area of these fibers benefits their interactions with the UHPC cementitious matrix. When compared with the 'UHPC-B4a' mix in Group #1, The 'UHPC-B5a' mix provided slightly better fresh mix workability with straight steel fibers used at the same dosage (1.0 vol%) in the "UHPC-B4a" mix in Group #1. This allowed for increasing the fiber dosage to 1.5 vol% with a minor rise in the HRWR dosage. The 'UHPC-B5a' mix exhibited relatively low workability and compressive strength, except when for formulations made using crushed grained and natural sand from New Mexico, probably due to the high water absorption rates of the NM aggregates. The compressive strengths achieved with Group #2 mixtures were higher than those of Group #1, but still fell short of the minimum 150 MPa (22 ksi) requirment.

4.3 Quartz powder

Group #3 UHPC mixtures (Table 7) incorporated quartz powder with average particle size of 3.9 μm. The results shown in Table 7 indicate that the flowability of fresh 'UHPC-B6a' mix was slightly better than that of 'UHPC-B5a'. Furthermore, the compressive strength of 'UHPC-B6a' was 156 MPa (23 ksi), compared to 138 MPa (20 ksi) for 'UHPC-B5a'; this finding qualifies 'UHPC-B6a' as an UHPC. Group #3 mixtures also included a variation of a UHPC mix design [30] designated 'UHPC-B6b', where the limestone powder (which is not considered as cementitious materials and acts as filler) used in the original mix was replaced with quartz powder. When New Mexico aggregates were used in 'UHPC-B6a'

Table 5 The mix proportions (kg/m^3) and properties of Group #1 UHPC mixtures

Mix constituent	UHPC-B2	UHPC-B3	UHPC-B4a	UHPC-B4b
Aggregates	1281.7	1281.7	1281.7	1281.7
#6 Crushed granite	715.8	715.8	715.8	715.8
#9 Natural sand	565.9	565.9	565.9	565.9
Binder-to-aggregate ratio	0.75	0.75	0.75	0.75
Cementitious materials	961.3	961.3	961.3	961.3
Cement Type I	672.9	672.9	672.9	672.9
Silica fume	96.1	96.1	96.1	96.1
Slag	192.3	192.3	192.3	192.3
Water/binder ratio	0.19	0.17	0.17	0.18
Water	153.8	134.6	144.2	153.8
HRWR (Chryso 150)	46.1	40.4	28.8	30.8
Steel fiber (0.5/30 mm, hooked)	79.2	77.5	116.1	117.4
Flow table (cm) (static/dynamic)	25.0/27.0	21.0/23.0	16.5/18.5	24.0/28.0
Compressive strength (MPa) (7 days)	112.3	114.6	102.3	112.1
Compressive strength (MPa) (28 days)	115	117.4	103.2	114.8

Table 6 The proportions (kg/m^3) and properties of Group #2 UHPC mixtures

Mix constituent	UHPC-B4c	UHPC-B4d	UHPC-B5a	UHPC-B5b (NM)
Aggregates	1281.7	1281.7	1281.7	1281.7
#7 Crushed granite	715.8	640.8	715.8	715.8
#9 Natural sand	565.9	640.8	565.9	565.9
Binder-to-aggregate ratio	0.75	0.75	0.75	0.75
Cementitious materials	961.3	961.3	961.3	961.3
Cement Type I	672.9	672.9	672.9	672.9
Silica fume	96.1	96.1	96.1	96.1
Slag	192.3	192.3	192.3	192.3
Water/binder ratio	0.17	0.17	0.18	0.18
Water	144.2	144.2	144.2	144.2
HRWR (Chryso 150)	28.8	28.8	36.0	36.0
Steel fiber, straight (0.17/13 mm)	77.4	77.5	116.9	116.9
Flow table (cm) (static/dynamic)	17.5/19.0	17.5/18.0	20.0/23.0	10.0/14.0
Compressive strength (MPa) (7 days)	106.2	118.7	138.0	129.0
Compressive strength (MPa) (28 days)	109.0	120.4	143.2	133.8

Table 7 The mix proportions (kg/m^3) and properties of Group #3 mixtures

Mix constituent	UHPC-B6a	UHPC-B6b	UHPC-B10b (NM)	UHPC-B10c
Aggregates	1281.7	1426.3	1281.7	1281.7
#7 Crushed granite	715.8	855.4	715.8 (NM)	715.8 (#8)
#9 Natural sand	565.9	570.9	565.9 (NM)	565.9
Binder-to-aggregate ratio	0.75	0.58	0.75	0.75
Cementitious materials	961.3	834.1	961.3	961.3
Cement Type I	480.6	417.0	480.6	480.6
Silica fume	96.1	83.4	96.1	96.1
Slag	192.3	166.8	192.3	192.3
Quartz powder	192.3	166.8	192.3	192.3
Water/cementitious ratio	0.18	0.17	0.18	0.18
Water	144.2	125.1	144.2	144.2
HRWR (Chryso 150)	36.0	25.0	36.0	36.0
Steel fiber, straight (0.17/13 mm)	118.2	115.9	118.2	118.2
Flow table (cm) (static/dynamic)	20.5/22.5	21.0/23.0	10.0/14.0	22.0/24.0
Compressive strength (MPa) (7 days)	145.6	120.0	148.0	149.0
Compressive strength (MPa) (28 days)	146.8	123.6	151.2	154.3

(the 'UHPC-B10b' mix), the fresh mix flowability dropped significantly. In 'UHPC-B10c', the maximum size of coarse aggregates was reduced to ASTM C33 #8 (9.5 mm, 3/8 in); this significantly lowered the fresh mix flowability. In 'UHPC-B10c', the maximum size of coarse aggregate was reduced to 9.5 mm, 3/8 in (ASTM C33 #8); as a result, the fresh mix workability was improved, and so did the compressive strength of UHPC. The Group #3 mixtures provided higher compressive strengths than Group #2. With 7-day compressive strengths generally approaching 150 MPa, the long-term strength of most of Group

Table 8 The proportions (kg/m^3) and properties of Group #4 UHPC mixtures

Mix constituent	UHPC-B9a	UHPC-B9b	UHPC-B9c
Aggregates	1281.7	1281.7	1281.7
Crushed granite	715.8 (#7)	715.8 (#8)	715.8 (#8)
#9 Natural sand	565.9	565.9	565.9
Binder-to-aggregate ratio	0.75	0.75	0.75
Cementitious materials	961.3	961.3	961.3
Cement Type I	672.9	672.9	480.6
Silica fume	96.1	96.1	96.1
Fly ash	192.3	192.3	192.3
Quartz powder	–	–	192.3
Water/cementitious ratio	0.18	0.18	0.17
Water	144.2	144.2	144.2
HRWR (Chryso 150)	36.0	36.0	28.8
Steel fiber, straight (0.17/13 mm)	118.6	118.6	119.1
Flow table (cm) (static/dynamic)	20.0/23.0	22.0/24.0	21.0/23.0
Compressive strength (MPa) (7 days)	127.0	128.0	152.0
Compressive strength (MPa) (28 days)	132.1	133.5	154.7

#3 mixtures are expected to surpass 150 MPa (22 ksi), qualifying them as UHPC.

4.4 Fly ash versus slag

Ground granulated blast-furnace slag was replaced with fly ash (Class F) in Group # 4 mixtures (Table 8), with other constituents kept similar to those used in Group #2 and Group #3 mixtures. Unlike the rough and angular particles of ground granulated blast furnace slag, most fly ash particles are spherical. Replacement of angular ground granulated blast furnace slag particles with spherical fly ash particles may improve the fresh mix workability, and increase the packing density of UHPC. When compared with 'UHPC-B5a' and 'UHPC-B10c' mixtures in Group # 2 and 3, respectively, the 'UHPC-B9a' and 'UHPC-B9c' mixtures in Group #4 with fly ash show slightly improved flowability and compressive strength. These mixtures, however, still fell short of the targeted >150 MPa (>22 ksi) compressive strength.

4.5 Silica fume

Group #5 mixtures (Table 9) evaluate the effects of silica fume on the flowability and strength of UHPC. Higher silica fume contents are observed to reduce the fresh mix flowability, mostly due to the high specific surface area of silica fume. Additionally, compressive strength of concrete increased with increasing silica fume content. Further reduction of water or replacement of slag with fly ash produced additional gains in compressive strength. Seven-day strengths as high as 183.5 MPa were reached in Group #5 mixtures with thermal curing.

4.6 Optimization of grading

As noted earlier in discussions on "Continuously graded particle packing", mix designs were optimized based on the modified Andreassen model using the commercial software "EMMA". Group #6 mixes (Table 10) emphasized use of these mix design principles to achieve further gains in compressive strength. The optimized mix design ('Ideal 4') successfully raised the compressive strength of UHPC to 192.6 MPa (28 ksi) and 202.1 MPa (30 ksi) with NM and MI aggregates, respectively, at 7 days of age (with thermal curing). The values of distribution coefficient q in the modified Andreassen model was compared to the measured values of workability and strength in order to determine if the coefficient q can be used during the mix design as a means of optimizing the fresh mix workability and/or the strength of UHPC. Figure 6 suggests that there may be correlations between the q-value and the workability of the fresh mix as well as the compressive

Table 9 The proportions (kg/m^3) and properties of Group #5 mixtures

Mix constituent	UHPC-B11a	UHPC-B12b	UHPC-B12c	UHPC-B15a	UHPC-B18a
Aggregates	1281.7	1281.7	1281.7	1281.7	1281.7
Crushed granite	715.8 (#7)	715.8 (#7)	715.8 (#8)	715.8 (#7)	715.8 (#8)
#9 Natural sand	565.9	565.9	565.9	565.9	565.9
Binder-to-aggregate ratio	0.75	0.75	0.75	0.75	0.75
Cementitious materials	961.3	961.3	961.3	961.3	961.3
Cement Type I	480.6	480.6	480.6	480.6	480.6
Silica fume	144.2	192.3	192.3	192.3	192.3
Slag/Fly Ash	192.30 (S)	96.10(S)	96.10 (S)	96.10 (S)	96.10 (F)
Quartz powder	144.2	192.3	192.3	192.3	192.3
Water/cementitious ratio	0.18	0.18	0.18	0.17	0.17
Water	144.2	144.2	144.2	144.2	144.2
HRWR (Chryso 150)	36.0	36.0	36.0	36.0	36.0
Steel fiber, straight (0.175/13 mm)	118.8	119.7	119.7	119.7	119.7
Flow table (cm) (static/dynamic)	19.5/22.0	11.0/16.5	14.0/18.0	13.0/18.0	12.0/16.0
Compressive strength (MPa) (7 days)	156.2	163.0	162.8	177.0	183.5
Compressive strength (MPa) (28 days)	161.2	165.3	164.5	181.2	185.8

Table 10 The proportions (kg/m^3) and properties of Group #6 UHPC mixtures

Mix constituent	Ideal 1 UHPC-B11b	Ideal 2 UHPC-B11c	Ideal 4 UHPC-B12a	Ideal 4 UHPC-B16a	Ideal 4 UHPC-B18b
Aggregates	1281.7	1281.7	1281.7	1281.7	1281.7
Crushed granite	640.8	512.7	487.0	487.0 (NM)	487.0
#9 Natural sand	640.8	769.0	512.7	512.7	512.7
Silica sand	–	–	282.0	282.0	282.0
Binder-to-aggregate ratio	0.75	0.65	0.75	0.75	0.75
Cementitious materials	961.3	833.1	961.3	961.3	961.3
Cement Type I	480.6	416.5	480.6	480.6	480.6
Silica fume	192.3	166.6	211.5	211.5	211.5
Slag/fly ash	96.1	83.3	96.1	96.1	96.1
Quartz powder	192.3	166.6	173.0	173.0	173.0
Water/cementitious ratio	0.18	0.18	0.18	0.16	0.16
Water	144.2	125.0	144.2	144.2	144.2
HRWR (Chryso 150)	36.0	31.2	36.0	36.0	36.0
Steel fiber, straight (0.17/13 mm)	119.8	120.7	120.3	120.3	120.3
Flow (cm) (static/dynamic)	14.5/16.5	14.0/19.0	19.0/22.0	10.0/14.0	11.0/15.5
Compressive strength (MPa) (7 days)	164.0	161.9	168.7	192.6	202.1
Compressive strength (MPa) (28 days)	167.2	165.3	171.6	195.2	203.2

strength of the hardened UHPC. As the value of q decreased, fresh mix workability increased, and 7-day compressive strength also increased. In addition, other investigations have suggested that q values of 0.26–0.29 correspond to optimal workability of high-strength concrete [37]. The mix designs

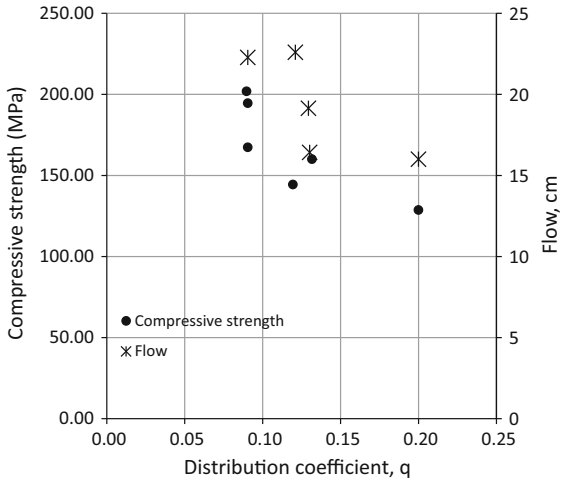

Fig. 6 Correlations of the distribution coefficient q with the fresh mix workability (flow) and the compressive strength of UHPC

developed here have much lower q values, but still offer desired flowability. The experimental results for Group #6 UHPC mixtures verified that the modified Andreassen model is a useful tool for design of UHPC mixtures.

4.7 Silica sand

It is generally believed that silica sand (>99.5 wt% SiO_2 with particle size of 0.1–0.5 mm) is a more suitable choice than natural sand for use in UHPC due to the purity, mechanical properties and fine dimensions of silica sand. The UHPC Group #7 mixtures included mix designs similar to those investigated earlier, except that natural sand was replaced with silica sand. Mixtures 'UHPC-B13a' and 'UHPC-B13b' were prepared without steel fibers in order to further reduce their water/binder ratios. These mixtures did not provide desired workability and compressive strength, which may be attributed to the deviation from a smooth grading of particulate matter.

4.8 Refinement of UHPC mix design

The UHPC mix designs were further refined (Table 11) towards realizing balanced improvements in fresh mix workability, compressive strength, and rate of hydration (and consequent heat release). These empirical refinements of the theoretical mix designs sought to produce an experimental data base on the

Table 11 Mix proportions (kg/m^3) and properties of refined theoretical UHPC mix designs

Mix constituent	UHPC-B20a	UHPC-B21a	UHPC-B20b	UHPC-B20c	UHPC-B21b	UHPC-B22a	UHPC-B22b
Total aggregates	1281.7	1281.7	1281.7	1281.7	1281.7	1281.7	1281.7
Crushed granite	487.0 (#8)	487.0 (#8)	487.0(#8)	487.0 (#7)	487.0 (#7)	487.0 (#8)	487.0 (#8)
#9 Natural sand	512.7	512.7	512.7	512.7	512.7	512.7	512.7
Silica sand	282.0	282.0	282.0	282.0	282.0	282.0	282.0
Binder ratio	0.75	0.75	0.75	0.75	0.75	0.75	0.75
Cementitious material	961.3	961.3	961.3	961.3	961.3	961.3	961.3
Cement Type I	480.6	480.6	384.5	480.6	480.6	480.6	384.5
Silica fume	211.5	211.5	211.5	211.5	211.5	211.5	192.3
Slag (S)/fly ash (F)	96.1 (S)	96.1 (F)	192.3 (F)	96.1 (S)	96.1 (S)	96.1 (S)	192.2 (S)
Quartz (Q)/limestone powder (LS)	173.0 (Q)	173.0 (Q)	173.0 (Q)	173.0 (LS)	173.0 (LS)	173.0 (LS)	192.2 (LS)
W/CM ratio	0.17	0.16	0.17	0.18	0.17	0.16	0.16
Water	132.7	129.8	132.7	144.2	132.7	132.7	132.7
HRWR	37.1	38.9	37.1	36.0	37.1	33.2	33.2
Steel fiber (0.17/13 mm)	119.1	118.9	121.1	120.3	119.1	118.6	118.7
Static/dynamic flow (cm)	17.5/19.0	16.0/18.5	17.0/19.5	20.5/24.0	20.5/23.5	17.5/18.5	20/21.5
Compressive strength (MPa) (7 days)	204.5 ± 8.2	195.8 ± 1.3	187.4 ± 3.8	183.8 ± 3.9	203.0 ± 3.1	195.2 ± 2.9	191.5 ± 8.6
Compressive strength (MPa) (28 days)	201.2 ± 6.5	197.5 ± 1.3	188.8 ± 8.3	189.4 ± 8.6	201.9 ± 4.7	191. ± 2.9	194.7 ± 2.9

effects of some material selection and mix design variables on the fresh mix workability and compressive strength of UHPC.

The effect of replacing ground granulated blast furnace slag with fly ash, as a pozzolanic constituent of the cementitious binder in UHPC, was evaluated. The UHPC mix 'UHPC-B21a' in Table 11, when compared with the 'UHPC-B21a' mix, incorporates Class F fly ash in lieu of ground granulated blast slag (in the cementitious binder composition).The spherical (and plerospherical) nature of fly ash particles (versus the angular nature of slag particles) allowed for further reduction of the water content of UHPC (although the superplasticizer content was raised slightly). The two mixtures provided comparable levels of fresh mix workability (measured by the static/dynamic flow table tests). The mix with fly ash ('UHPC-B21a'), in spite of its lower water/binder ratio, provided a slightly lower compressive strength when compared with the mix prepared with ground granulated blast furnace slag ('UHPC-B20a').

Micro-scale mineral powders are viewed here as constituents of the cementitious binder. This view is rationalized by the fact that, due to the relatively low water/binder ratio of UHPC, a significant fraction of cement remains unreacted and acts as a filler (with strong interfacial bonding) within the cured UHPC. Hence, replacement of a fraction of cement with higher-performance mineral powder could benefit the performance characteristics of UHPC. Some mineral powders are also found to accelerate hydration of cement by lowering the water/binder ratio and enhancing heterogeneous nucleation of hydration products on the high surface area of powder particles [40]. An empirical assessment was made of the effects of the type of mineral powder on the fresh mix and hardened material properties of UHPC. Two mineral powders were considered here: limestone with a greater potential for reactive interfacial bonding to cement hydrates, and quartz with higher inherent mechanical properties. Yahia et al. showed that partial replacement of cement with an equal volume of limestone powder (500–1000 m^2/kg specific surface area) lowered the yield stress of a fresh cementitious mortar, producing a highly flowable mixture [41]. Other investigations have shown that partial (5–20 %) replacement of cement with an equal volume of limestone powder benefits the fluidity of high-performance concrete with water/binder ratios ranging from 0.35 to 0.41 [42]. Such improvements in fresh mix workability may have resulted from a rise in the water/binder ratio of paste as a result of partial replacement of cement with limestone powder. It is worth mentioning that, due to the differences in density of limestone powder and cement, partial replacement of cement with limestone on an equal mass basis would increase the volume of paste in mix.

Limestone powder (acquired from Betocarb HP-PT, OMYA A.G.) was used to replace quartz flour in the 'UHPC-B20c' mix, with other constituents kept similar to those in the 'UHPC-B21b' UHPC mix (Table 11). The superior fresh mix workability of the 'UHPC-B20C' mix with limestone powder allowed for further reduction of water/binder ratio. In spite of this, the 'UHPC-B21b' mix with limestone powder still provided higher workability (static/dynamic flow table test results of 20.5/23.5) than the 'UHPC-B20a' mix (17.5/19 cm) made with quartz powder (and higher water/binder ratio). Both these mixtures provided compressive strengths exceeding 200 MPa (30 ksi). Oey et al. suggest that limestone is more effective than quartz (and some other fillers) as an accelerator due to its interfacial properties and its ability to participate in ion-exchange reactions [40]. In the presence of limestone powder, calcium aluminate monocarbonate is formed preferably, hydration of C_3S is accelerated, and some carbosilicates also tend to be form [43]. Other investigations have shown that the presence of limestone powder in the cementitious binder benefits the dispersion and compaction of the particulate matter, precipitation of $Ca(OH)_2$ and C-S–H gel, and formation of crystalline matter [44]. The specifics of concrete mix design can influence the effects of limestone powder on compressive strength [41].

Given the desired fresh mix workability of 'UHPC-B21b', the 'UHPC-B22a' mix in Table 11 was reproduced with reduced superplasticizer (HRWR) content (and thus reduced cost). This change, however, compromised not only the fresh mix workability but also the compressive strength of this UHPC mix.

Due to concerns with the high cement content and thus the potential for high heat of hydration of UHPC, an attempt was made to increase the slag content of the cementitious binder from 10 to 20 % (reducing the cement content from 50 to 40 %), yielding the 'UHPC-B22b' mix in Table 11. In spite of desired fresh mix workability, the compressive strength of 'UHPC-B22b' failed below 200 MPa (30 ksi).

The experimental results discussed above (and summarized in Table 11), using different empirical variations of the theoretical UHPC mix, indicated that the 'UHPC-B21b' mix in Table 11 is the preferred mix design at this stage of development, offering desired fresh mix workability and about 200 MPa (30 ksi) compressive strength.

5 Pilot scale production of UHPC in the field

5.1 Materials and methods

In a ready-mixed concrete plant, UHPC the mixture of UHPC-B21b in Table 11 was produced, with a total volume of 1.33 m^3 (1.74 yd^3).

The following sequence of batching and mixing was selected:

- Automated batching of 50 % of granite coarse aggregate, all of the natural sand fine aggregate, silica sand, cement, slag, silica fume, and 50 % of water and superplasticizer (with mixer rotating at 15 revolutions/min);
- Manual addition (of limestone powder);
- Automated batching of the remaining 50 % of granite coarse aggregate, water, and superplasticizer (with mixer rotating at 15 revolutions/min);
- Manual addition of steel fiber and set retarder followed by thorough mixing, and final checking of fresh mix prior to delivery.

The UHPC mix was cast directly from the concrete truck into the formwork prepared for production of blocks. Following internal consolidation and surface finishing of the UHPC blocks, their exterior surfaces were covered with concrete curing (insulating) blanket. The reinforcement cage and the wooden formwork were used for production of the larger reinforced UHPC 1 m × 1 m × 1 m (3.3 ft × 3.3 ft × 3.3 ft) block. The readily available concrete curing (insulating) blanket used to facilitate effective use of the heat of hydration of the cementitious binder in UHPC towards field thermal curing of the block provided an insulation value of $R = 7.0$.

Four thermocouples were placed inside each UHPC block for monitoring of temperatures near bottom, center and top (all central region) as well as side (mid-height near wooden formwork) of the block over time. Ambient temperature was also monitored.

An important consideration in scaled-up production of UHPC is the precision in batching of different mix ingredients. The relatively low water content of UHPC as well as the sensitivity of UHPC compressive strength to water/binder ratio require careful control of the water content and also the cementitious binder content of the mix. The precision of the instruments used for automated batching of the mix ingredients in the ready-mixed concrete plant together with the fact that a relatively small quantity of UHPC (accounting for only 15 % of the tuck capacity) was considered, it produced up to 10 % deviation from the targeted water and cementitious contents of UHPC. These deviations could be lowered below 2 % if 70 % of the truck capacity was batched (which is the common practice).

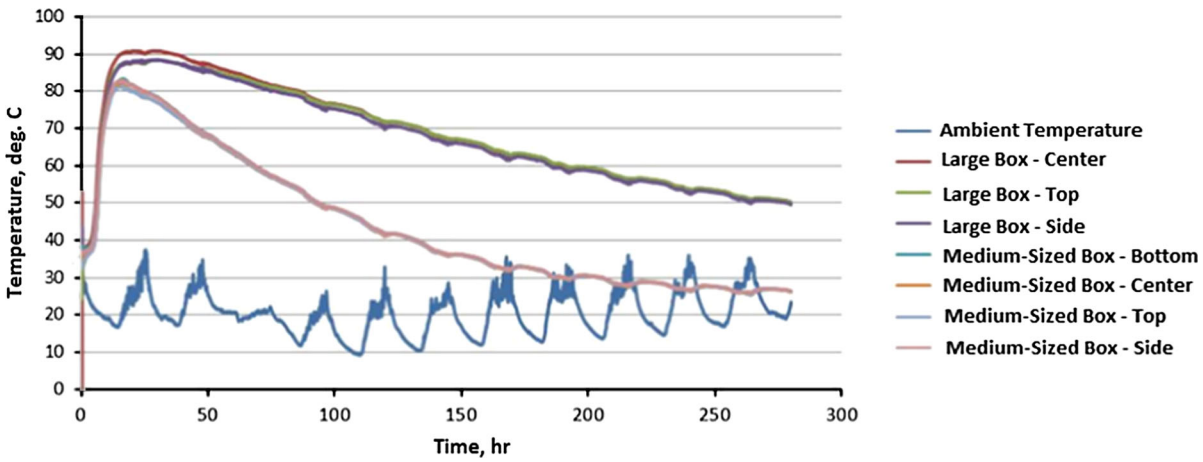

Fig. 7 Temperature time histories at different locations within the large and medium-sized blocks made with the UHPC prepared at pilot scale

An important note from the pilot-scale investigation was that the 10 % deviation from the targeted water and cement contents when only 15 % of the truck capacity was batched compromised the fresh mix workability. The lack of precision in automated batching of this relatively small quantity of UHPC in ready-mixed concrete plant required a rise in the superplasticizer (HRWR) content by 10 % of the originally targeted level in order to achieve an acceptable fresh mix workability marked by 279 mm (1 in) slump and 610 mm (24 in) slump flow. This desired fresh mix workability facilitated convenient casting, consolidation and finishing of the relatively large UHPC blocks in a sunny day with measured site temperature of 30 °C (86 °F).

5.2 Field evaluation of the large UHPC structure

The temperature time-histories recorder at different locations of the large (1 m × 1 m × 1 m) and medium-sized (0.3 m × 0.3 m × 0.3 m) blocks are shown in Fig. 7 together with the measured values of ambient temperature, which varied from 10 to 35 °C (50–95 °F). The temperature time-histories obtained within the medium-sized block made with UHPC produced at pilot scale were comparable to those obtained for similar blocks made earlier using the UHPC produced in laboratory. Temperatures measured at different locations within the medium-sized UHPC block exhibited at a reasonable uniform distribution of temperature within the volume; a peak temperature of 80 °C (176 °F) was reached after 12 h; subsequently, temperature dropped gradually, and it took 96 h to drop to 50 °C (122 °F). This is a favorable temperature time-history for thermal curing of UHPC. In the case of the large 1 m × 1 m × 1 m (3.3 ft × 3.3 ft × 3.3 ft) UHPC block covered with concrete curing (insulating) blanket, temperature within the volume rose uniformly to 90 °C (194 °F) within 13.5 h, and remained above 70 °C (158 °F) for more than 100 h. This is a highly desirable temperature time-history for thermal curing of UHPC. The higher peak temperature and slower temperature drop in the large UHPC block, when compared with the medium-sized block, points at the reduced rate of heat loss (per unit volume) from the larger block. This can be attributed to the smaller surface-to-volume ratio of the larger block.

Due to the imprecise batching of the relatively small quantity (15 % of truck capacity) of UHPC at the ready-mixed concrete plant, cylinders made directly from the UHPC truck and cured at 90 °C (194 °F) over 48 h showed 7-day compressive strengths of 159 ± 4 MPa (23.0 ± 0.6ksi), compared to >200 MPa (30ksi) compressive strength obtained with the same UHPC mix produced in laboratory. Cores extracted from the large concrete block which experienced a particularly favorable temperature time-history (using the heat of hydration of cementitious binder, without any external heating) produced compressive strengths of 167 ± 6 MPa (24.2 ± 0.9ksi), which exceeded the strengths produced with controlled thermal curing in laboratory. This confirms the desired thermal curing condition within the large concrete block generated by the heat of hydration of the UHPC cementitious binder (in the presence of a set retarder). Still, the inaccurate batching of the relatively small volume of UHPC in the ready-mixed concrete plant lowered the 7-day compressive strength of the pilot-scale UHPC below the >200 MPa (30ksi) obtained in laboratory-scale production. An evaluation of the batching operation in the ready-mixed concrete plant indicated that production of 70 % of truck capacity (10 yd^3) versus the 15 % truck capacity prepared in the pilot-scale investigation alone could yield the precision needed to reproduce the success in laboratory-scale preparation of UHPC which reached the targeted 200 MPa (30ksi) compressive strength. The favorable curing conditions within large UHPC structures produced compressive strengths which exceeded that obtained with controlled thermal curing in laboratory. The favorable moisture condition within the large structure will also help improve the UHPC strength over longer time periods.

6 Conclusions

The primary goal of this study is to develop mix design procedures and production methods for reliable construction of large UHPC using locally available materials and concrete-making facilities. Compressive strengths above 200 MPa (30 ksi) are targeted. Criteria were developed for selection of local materials to be used in UHPC structures. The linear packing density model and the continuously

graded particle packing model provided the theoretical basis for proportioning the UHPC mixtures. After comprehensive experimental study on trial mixes and incorporation of the lessons learned into the mix design procedures, final UHPC mix designs were developed. Finally, pilot-scale field study was conducted where UHPC was produced in a ready-mixed concrete plant. The final UHPC mix design developed in the study was used for pilot-scale production of a large 1 m × 1 m × 1 m (3.3 ft × 3.3 ft × 3.3 ft) reinforced concrete block, with UHPC batched in a ready-mixed concrete plant and mixed/transported using a conventional concrete truck (transit mixer). The mixing process was reasonably successful, and the fresh mix provided desired workability characteristics. Placement and consolidation of UHPC in the large form with steel reinforcement was successful. The temperature time-histories monitored at different locations within the block covered with a readily available insulating blanket indicated a uniform temperature rise that suits thermal curing of UHPC.

Acknowledgments The authors wish to acknowledge the support of U.S. Air Force (Award FA9550-13-C-0029) for the project reported herein.

References

1. Habel K, Viviani M, Denarie E, Bruhwiler E (2006) Development of the mechanical properties of an ultra-high performance fiber reinforced concrete (UHPFRC). Cem Concr Res 36(7):1362–1370
2. Wille K, Naaman AE, El-Tawil S, Parra-Montesinos GJ (2011) Ultra-high performance concrete and fiber reinforced concrete: achieving strength and ductility without heat curing. Mater Struct 45(3):309–324
3. Corinaldesi V, Moriconi G (2012) Mechanical and thermal evaluation of ultra high performance fiber reinforced concretes for engineering applications. Constr Build Mater 26(1):289–294
4. Ahlborn TM (2012) Ultra-high performance concrete. National Precast Concrete Association
5. Akhnoukh AK, Xie H (2010) Welded wire reinforcement versus random steel fibers in precast/prestressed ultra-high performance concrete I-girders. Constr Build Mater 24(11):2200–2207
6. Bornemann R, Schmidt M (2002) Ultra high performance concrete (UHPC)—mix design and application. Concr Precast Plant Technol 68(2):10–12
7. Garas VY, Kurtis KE, Kahn LF (2012) Creep of UHPC in tension and compression: effect of thermal treatment. Cem Concr Compos 34(4):493–502
8. Grunewald S, Van Loenhout P (2008) Application of ultra high performance concrete outstanding projects from hurks beton. Concr Plant Precast Technol 74(11):26–34
9. Habel K, Charron J-P, Braike S, Douglas Hooton R, Gauvreau P, Massicotte B (2008) Ultra-high performance fibre reinforced concrete mix design in central Canada. Can J Civ Eng 35(2):217–224
10. Yang SL, Millard SG, Soutsos MN, Barnett SJ, Le TT (2009) Influence of aggregate and curing regime on the mechanical properties of ultra-high performance fibre reinforced concrete (UHPFRC). Constr Build Mater 23(6):2291–2298
11. Skazlic M, Ille K, Ille M (2012) UHPFRC composition optimization for application in rehabilitation of RC structures. In: 4th International conference on concrete repair, 26–28 Sept, 2011. Taylor and Francis, Dresden, pp 795–802
12. Koh K-T, Park J-J, Kang S-T, Ryu G-S (2012) Influence of the type of silica fume on the rheological and mechanical properties of ultra-high performance concrete. In: 10th International conference on fracture and damage mechanics (FDM2011), 19–21 Sept 2011. Trans Tech Publications, Dubrovnik, pp 274–277
13. Barnett SJ, Lataste J-F, Parry T, Millard SG, Soutsos MN (2010) Assessment of fibre orientation in ultra high performance fibre reinforced concrete and its effect on flexural strength. Mater Struct 43(7):1009–1023
14. Kang S-T, Kim J-K (2011) The relation between fiber orientation and tensile behavior in an ultra high performance fiber reinforced cementitious composites (UHPFRCC). Cem Concr Res 41(10):1001–1014
15. Kang S-T, Kim J-K (2012) Numerical simulation of the variation of fiber orientation distribution during flow molding of ultra high performance cementitious composites (UHPCC). Cem Concr Compos 34(2):208–217
16. Soliman AM, Nehdi ML (2011) Effect of drying conditions on autogenous shrinkage in ultra-high performance concrete at early-age. Mater Struct 44(5):879–899
17. Lei Voo Y, Foster SJ (2010) Characteristics of ultra-high performance 'ductile' concrete and its impact on sustainable construction. IES J Part A 3(3):168–187
18. Toledo Filho RD, Koenders EAB, Formagini S, Fairbairn EMR (2011) Performance assessment of ultra high performance fiber reinforced cementitious composites in view of sustainability. Mater Des 36:880–888
19. Van Tuan N, Ye G, Van Breugel K, Fraaij ALA, Bui DD (2011) The study of using rice husk ash to produce ultra high performance concrete. Constr Build Mater 25(4):2030–2035
20. Dils J, Boel V, De Schutter G (2013) Influence of cement type and mixing pressure on air content, rheology and mechanical properties of UHPC. Constr Build Mater 41:455–463
21. Peyvandi A, Soroushian P, Lu J, Balachandra AM (2014) Enhancement of ultrahigh performance concrete material properties with carbon nanofiber. Adv Civ Eng
22. Sbia LA, Peyvandi A, Soroushian P, Balachandra AM, Smith I (2014) Optimization of ultra-high-performance concrete with nano-and micro-scale reinforcement. Cogent Eng 1(1):990673
23. Sbia LA, Peyvandi A, Soroushian P, Balachandra AM, Sobolev K (2015) Evaluation of modified-graphite

nanomaterials in concrete nanocomposite based on packing density principles. Constr Build Mater 76:413–422
24. Malekmotiei L, Samadi-Dooki A, Voyiadjis GZ (2015) Nanoindentation study of yielding and plasticity of poly (methyl methacrylate). Macromolecules 48(15):5348–5357
25. Peyvandi A, Soroushian P (2015) Structural performance of dry-cast concrete nanocomposite pipes. Mater Struct 48(1–2):461–470
26. Mazanec O, Lowke D, Schiel P (2010) Mixing of high performance concrete: effect of concrete composition and mixing intensity on mixing time. Mater Struct 43(3):357–365
27. Tam C-M (2012) Tam VW-Y. Microstructural behaviour of reactive powder concrete under different heating regimes. Mag Concr Res 64(3):259–267
28. de Larrard F, Sedran T (1994) Optimization of ultra-high-performance concrete by the use of a packing model. Cem Concr Res 24(6):997–1009
29. Mehta PK, Monteito PJM (2006) Concrete microstructure, properties, and materials, 3rd edn. McGraw-Hill, New York
30. Wang C, Yang C, Liu F, Wan C, Pu X (2012) Preparation of ultra-high performance concrete with common technology and materials. Cem Concr Compos 34(4):538–544
31. Park SH, Kim DJ, Ryu GS, Koh KT (2012) Tensile behavior of ultra high performance hybrid fiber reinforced concrete. Cem Concr Compos 34(2):172–184
32. de Larrard F, Sedran T (2002) Mixture-proportioning of high-performance concrete. Cem Concr Res 32(11):1699–1704
33. Amirjanov A, Sobolev K (2008) Optimization of a computer simulation model for packing of concrete aggregates. Part Sci Technol 26(4):380–395
34. Elkem. User Guide to Elkem Materials Mixture Analyser—EMMA, Program Version 3.5.1
35. Dinger DR, Funk JE (1992) Discrete versus continuous particle sizes. Interceramics 41(5):332–334
36. Husken G (2010) A multifunctional design approach for sustainable concrete—with application to concrete mass products. Eindhoven University of Technology
37. Garas VY, Kurtis KE (2008) Assessment of methods for optimising ternary blended concrete containing metakaolin. Mag Concr Res 60(7):499–510
38. Ma J, Schneider H (1200) Properties of ultra-high-performance concrete. Leipzig Annual Civil Engineering Report (LACER), No. 7, pp 5–32
39. Maruyama I, Teramoto A (2013) Temperature dependence of autogenous shrinkage of silica fume cement pastes with a very low water–binder ratio. Cem Concr Res 50:41–50
40. Oey T, Kumar A, Bullard JW, Neithalath N, Sant G (2013) The filler effect: the influence of filler content and surface area and cementitious reaction rates. J Am Ceram Soc 96(6):1978–1990
41. Yahia A, Tanimura M, Shimoyama Y (2005) Rheological properties of highly flowable mortar containing limestone filler-effect of powder content and W/C ratio. Cem Concr Res 35(3):532–539
42. Nehdi M, Mindess S, Aitcin PC (1998) Rheology of high-performance concrete: effect of ultrafine particles. Cem Concr Res 28(5):687–697
43. Kakali G, Tsivilis S, Aggeli E, Bati M (2000) Hydration products of C(3)A, C_3S and Portland cement in the presence of $CaCO_3$. Cem Concr Res 30(7):1073–1077
44. Nehdi M, Mindess S, Aitcin PC (1996) Optimization of high strength limestone filler cement mortars. Cem Concr Res 26(6):883–893